



Published in final edited form as:

Lab Invest. 2021 June ; 101(6): 745–759. doi:10.1038/s41374-021-00534-4.

Forkhead box F1 induces columnar phenotype and epithelial-to-mesenchymal transition in esophageal squamous cells to initiate Barrett's like metaplasia

Alok De^{1,2}, **Jianping Zhou**^{1,2}, **Pi Liu**³, **Manling Huang**³, **Sumedha Gunewardena**^{4,5,7}, **Sharad C. Mathur**⁶, **Lane K. Christenson**^{5,7}, **Mukut Sharma**^{1,2}, **Qiuyang Zhang**^{3,*}, **Ajay Bansal**^{1,7,8,*}

¹Division of Gastroenterology and Hepatology, Veterans Affairs Medical Center, Kansas City, MO

²Midwest Biomedical Research Foundation (MBRF), Kansas City VA Medical Center, Kansas City, MO

³Department of Medicine, Center for Esophageal Diseases, Baylor University Medical Center and Center for Esophageal Research, Baylor Scott & White Research Institute, Dallas, Texas 75246, USA

⁴Bioinformatics Core Facility, University of Kansas, Kansas City, KS

⁵Department of Molecular and Integrative Physiology, University of Kansas Medical Center, Kansas City, KS

⁶Department of Anatomic Pathology and Laboratory Medicine, Veterans Affairs Medical Center and University of Kansas Medical Center, Kansas City

⁷Kansas Cancer Institute, Kansas City, KS

⁸Division of Gastroenterology and Hepatology, University of Kansas Medical Center, Kansas City, KS

Abstract

Multiple genome-wide association studies (GWAS) studies have linked Forkhead Box F1 (FOXF1) to Barrett's esophagus (BE). Understanding whether FOXF1 is involved in initiation of Barrett's metaplasia could allow FOXF1 to be used for risk stratification and for therapy. Two-dimensional cell cultures and 3-dimensional organoid cultures and well-annotated human biopsies were used to determine the role of FOXF1 in BE pathogenesis. Multiple established esophageal squamous and BE cell lines were tested in gain- and loss-of-function studies. Initiation of a BE like metaplastic change was evaluated by measuring characteristic cytokeratins and

***Co-corresponding authors: Ajay Bansal, MD**, Associate Professor of Medicine, University of Kansas School of Medicine, 3901 Rainbow Blvd., Kansas City, MO 66160; abansal@kumc.edu; Telephone: 913 588 6003; **Qiuyang Zhang, PhD**, Associate Professor of Medicine, Center for Esophageal Diseases, Baylor University Medical Center and Center for Esophageal Research, Baylor Scott & White Research Institute, Dallas, Texas 75246; qiuyangd.zhang@gmail.com; Telephone: 214 818 3150.

Author Contributions

Study concept and design: AB, QZ; Acquisition of data: AD, JZ, SM, PL, MH, QZ, MS; Analysis and interpretation of data: AD, AB, MS, LKC, SG, SM, PL, QZ; Drafting of the manuscript: AD, QZ, AB; Critical revision of the manuscript for important intellectual content: LKC, MS, QZ, AB; Statistical analysis: SG; Study supervision: QZ, LKC, AB

None of the authors have any conflicts of interest to declare.

Supplementary information is available at Laboratory Investigation's website.

global gene expression profiling and by culturing organoids. Epithelial-mesenchymal transition (EMT) was evaluated by immunostaining for E-cadherin, vimentin and Snail, and by cell motility assay. Columnar esophageal epithelium of BE patients exhibited higher expression of FOXF1 compared to normal squamous esophageal epithelium of GERD patients ($P < 0.001$). Acidic bile salts induced nuclear FOXF1 in esophageal squamous cells. FOXF1 overexpression in normal esophageal squamous cells: a) increased columnar cytokeratins and decreased squamous cytokeratins, b) converted squamous organoids to glandular organoids and c) switched global gene profiles to resemble that of human BE epithelium ($P = 2.1685 \times 10^{-6}$ for upregulated genes and $P = 8.3378 \times 10^{-9}$ for downregulated genes). FOXF1 inhibition in BE cell lines led to loss of BE differentiation markers, CK7 and mucin 2. Also, FOXF1 induced EMT and promoted cell motility in normal esophageal squamous epithelial cells. FOXF1 induced genes mapped to pathways such as Cancer, Cellular Assembly and Organization, DNA Replication, Recombination, and Repair. In conclusion, FOXF1 promotes a BE like columnar phenotype and cell motility in esophageal squamous epithelial cells, which may have a critical role in BE development. FOXF1 should be studied further as a biomarker for BE and as a target for BE treatment.

Keywords

FOXF1; Barrett's esophagus; esophageal adenocarcinoma; metaplasia

Introduction

The annual incidence of esophageal adenocarcinoma (EAC) in white men with Barrett's esophagus (BE) has increased by 10-fold from 0.6/100,000 to 6/100,000 over the past 40 years.¹ Although the risk is lower in other cohorts, the risk has continued to increase annually by 2.9% in women.² Most disturbing is the fact that the largest increase was seen in age groups younger than 50, in both men and women.² Other data have highlighted the alarming statistic that by 2030, 1 in 100 men in the developed world may be at risk for esophageal adenocarcinoma (EAC).³ Also, the survival rates have improved only marginally with ~81% dying within five years.⁴ The primary pathway to EAC is via Barrett's esophagus (BE), a metaplastic response to gastroesophageal reflux disease (GERD). Understanding molecular mechanisms behind BE development can help us understand the natural history of this disease and may lead to novel therapies to halt the rapid increase in EAC rates. There are multiple theories for origin of BE: squamous-to-columnar transdifferentiation or transcommitment, extension of submucosal glands and cell migration from the gastroesophageal junction to include gastric cardia stem cells⁵ or transitional basal cells⁶ or residual embryonic cells.⁷ Implicit in all of these models are the concepts of reflux-induced damage and wound healing that create opportunities for the development of BE.⁸

Several large-scale population genetics studies have found *FOXF1* to be significantly associated with BE and its complication, EAC, in white⁹⁻¹⁷ as well as non-white populations.¹⁸ *FOXF1* belongs to the forkhead box (FOX) family of transcriptional regulators characterized by a distinct forkhead DNA-binding domain.¹⁹ Various FOX proteins exhibit transcriptional plasticity that allows them to regulate gene activation,

transcriptional repression and modulation of epigenetic factors.¹⁹ This versatility enables FOX family to determine cell fate in various biological systems. *FOXF1* gene is highly conserved across species and implicated in embryonic digestive tract morphogenesis.²⁰ Deletion of *FOXF1* gene cluster is associated with developmental anomalies of the esophagus.²¹ A recent study showed that esophageal atresia can increase the risk of BE by four-fold suggesting that genes important in esophageal development may be linked to BE development.²² *FOXF1* may be a common link. Importantly, although multiple transcription and growth factors have been previously implicated in BE development,²³⁻²⁹ *FOXF1* may be particularly important because of its newly recognized status as a pioneer factor,^{30, 31} one that may promote the activity of other transcription factors in determining cell lineage by improving chromatin accessibility. The role of *FOXF1* in BE development is poorly understood. We used a combination of human material, gain-of-function and loss-of-function studies in well-established *in vitro* models to evaluate the role of *FOXF1* in BE development. Although several groups of investigators have reported strong association of *FOXF1* with BE and EAC in epidemiologic studies, to the best of our knowledge, our study is the first to investigate the functional effects of *FOXF1* in BE development.

Materials and Methods

Human studies

Procurement of human specimens and disease definitions—Participants were randomly selected from an ongoing repository of patients with BE and related conditions.^{32, 33} The repository has been reviewed and approved by the local Institutional Review Board annually and allows the collection of clinical data, tissue and serum specimens from patients with GERD and BE. All patients sign informed consent prior to enrollment. To maintain confidentiality, each patient is assigned a unique study number that does not use any of the 18 identifiers outlined in the institutional guidelines. GERD is defined on the basis of a validated questionnaire that systematically enquires about the presence of heartburn and regurgitation. Patients with GERD were further subclassified as the ones with erosive esophagitis (EE) and the others with non-erosive reflux disease (NERD). BE is defined by a) presence of columnar lined esophagus at least 1 cm in length and b) intestinal metaplasia in biopsies. In BE patients we obtain 1-2 biopsies every two cm from the Barrett's segment and 1-2 biopsies from the squamous esophagus two cm proximal to the proximal extent of BE. In GERD patients, we obtain 1-2 biopsies one cm and five cm above the gastroesophageal junction. All biopsies are bisected, and one piece is placed in formalin for histology and the other piece is placed in RNAlater or is snap frozen in liquid nitrogen for molecular studies. All specimens for molecular studies are stored at -80 degrees C.

Histologic evaluation of human specimens—All biopsies were reviewed by an experienced gastrointestinal pathologist according to the criteria outlined by Montgomery et al.,³⁴ as has been done for multiple previous studies.^{35, 36} Intestinal metaplasia was confirmed by the presence of goblet cells. If dysplasia was detected, a second experienced gastrointestinal pathologist reviewed the biopsies. A final diagnosis was reached by consensus, if there was disagreement.

Molecular evaluation of human specimens—We included those BE specimens with histologically confirmed intestinal metaplasia but without dysplasia. For GERD biopsies, we included the biopsy specimens obtained from the squamous esophagus one cm above the gastroesophageal junction. We chose the one cm rather than five cm location because acid and bile exposure would be higher at the one cm location. We measured *FOXF1* gene expression using qPCR and FOXF1 protein using immunohistochemistry. These methods are described below.

In vitro experiments

The conversion of squamous cells to a Barrett's like metaplastic morphology was evaluated by measuring the expression of specific BE associated columnar cytokeratin markers (CK7, CK20, Muc2) and squamous cytokeratin markers (CK10 and CK13), by qPCR, IHC and IF. Also, we measured global changes in *FOXF1* transfected cells (in triplicate) by next generation sequencing (details below) and compared them to differentially expressed genes between GERD and BE patients. To evaluate the potency of *FOXF1* transfection, we performed dose-dependent *FOXF1* transfection after serial dilution by a factor of 10 (up to 10⁴-fold). The cytokeratin-based endpoints were measured at each concentration. The experimental techniques are described below.

Cell culture—Multiple established cell lines were used, normal esophageal squamous cell lines: EPC2 (kind gift from Anil Rustgi, University of Pennsylvania, PA), NES-B10 and NES-G4 (kind gift from Souza lab, Baylor Scott & White, TX) and Het1-A (ATCC, Manassas, VA and BE cell lines, BAR-T (kind gift from Souza lab, Baylor Scott & White, TX). Culture conditions for the aforementioned cell lines have been previously described.³⁷⁻⁴⁰ All cell lines were maintained at 37°C in 5% carbon dioxide.

Acid and bile treatment—To mimic epithelial cell exposure to reflux condition (i.e., acid/bile),⁴¹⁻⁴³ normal esophageal squamous cell lines were treated with acid and bile salts (deoxycholic acid (Calbiochem, catalog# 264101), taurochenodeoxycholic (Calbiochem, catalog#580217)) and glycocholic (Calbiochem, catalog# 360512) acids. Bile acid mixture contained these bile salts in 1:1:1 ratio with concentrations ranging from 50 to 400 μM. To determine the conditions for acid and bile exposure, cells were exposed to varying pH and/ bile salt concentrations. Cell viability was measured using the MTT assays to determine the conditions that the cells could tolerate with <10% loss (Supplementary Data 1). Based on the above data, in all experiments, cells were treated with acid at pH 5.5 for 30 minutes or acidic bile (100 μM @ pH 5.5) for 30 minutes because lower pH or higher acidic bile concentrations led to >10% cell loss. This bile salt concentration is within the range of bile acid concentrations (30-820 μM with a median range of approximately 200 μM) seen clinically in the refluxed gastric juice in BE patients.⁴¹⁻⁴³

FOXF1 overexpression—Plasmid construct for *FOXF1* was generated at KanPro Research Inc. at the University of Kansas, Lawrence, KS (product details in Supplementary Data 1). Briefly, *FOXF1* DNA template was purchased from GE Health Care. *FOXF1* gene was amplified by PCR using primers that introduced NheI and XhoI restriction sites at the 5' and 3' end of the targeted gene, respectively. Both PCR products and the pCMV6-

AC-IRES-GFP vector were digested with the NheI and XhoI restriction enzymes. The inserts were ligated into the vector and the construct was confirmed by DNA sequencing at GenScript, Inc. The vector, pCMV6-AC-IRES-GFP, without inserts, was the empty vector. Cells were transfected with *FOXF1* plasmid or empty vector by using Lipofectamine 2000 (Life Technologies, Carlsbad, CA). Dose-dependent *FOXF1* transfection after serial dilution by a factor of 10 (up to 10⁴-fold) from 4.0 µg to 0.0004 µg was performed to determine the plasmid dose that led to *FOXF1* fold changes in vitro similar to those seen in human specimens.

We also generated stable esophageal squamous cell lines that overexpressed *FoxF1*. We transduced NESG4 cells with lentiviral particles carrying the corresponding cDNA and GFP (Cat# RC218259L2V, Origene, Rockville, MD). Three days after transduction, GFP-positive cells were sorted out by BD FACS Aria II sorter (BD Bioscience, San Jose CA) as previously done.⁴⁴ *FOXF1* overexpression in the repopulated cells was confirmed by western blotting.

FOXF1 inhibition—To inhibit *FOXF1*, BAR-T cells (patient-derived BE cell line) were transduced with four different GFP-tagged *FOXF1* shRNA viral particles versus scrambled non-target shRNA (Cat# TL312936V, OriGene). The knockdown efficiency was examined by western blotting. For immunofluorescent staining and stable cell line construction, cells were transduced with a mixture of these four viral particles. Three days after transduction, GFP-positive cells were sorted by flow cytometry.

3-Dimensional organoid culture—We followed an established method to cultivate organoids from normal squamous esophageal epithelial cells.⁴⁵ Two thousand NESG4 cells were resuspended in 25 µl of growth factor reduced matrigel (cat#356231, Corning, New York) before being seeded into a 48-well plate. This 3D culture was maintained in keratinocyte-SFM (KSFM) medium with supplementation of 50 µg/ml of bovine pituitary extract, 1 ng/ml EGF, and 0.6 mM calcium chloride. Medium was changed every two days until harvest. The culture was monitored daily for two weeks before harvest.

Immuno-staining of cultured cells—Immunocytochemistry was performed using our previously described methods.⁴⁶ Cells were fixed in 4% buffered formaldehyde, washed in phosphate buffered saline (PBS), and incubated with primary antibodies (Supplementary Data 1) overnight at 4°C. For immunofluorescent staining, we followed our published method⁴⁴ using antibodies listed in supplementary Table 1. Immunoassays were performed using ImmPRESS HRP reagent kit (Vector Laboratories, Burlingame, CA, USA) per the manufacturer's protocol. Cells were counterstained with hematoxylin. A Leica digital microscope was used for imaging.

Immunohistochemistry of tissue sections—Immunohistochemistry was performed as previously described.⁴⁶ Briefly, five µM tissue sections fixed in 4% buffered formalin were deparaffinized, rehydrated using decreasing concentrations of alcohol, washed with PBS and exposed to blocking serum (ImmPress, Vector Laboratories, Burlingame, CA). The treated sections were then incubated with appropriate antibodies (Supplementary Data 1) overnight in a humid chamber at 4°C. Immunoreactivity was detected using streptavidin-

conjugated secondary antibodies (ImmPRESS, Vector Laboratories) and counterstained with hematoxylin. The stained sections were imaged with a digital microscope (Leica Microsystems, Buffalo Grove, IL). Negative controls with omission of the primary antibody were included. Sections of kidney tubules served as positive controls as suggested by the manufacturer. All sections were scored by two gastrointestinal pathologists experienced in immunohistochemical evaluation. A scoring system was adapted from a previously published score.⁴⁷ Epithelial and stromal cells were separately scored: 0, no staining or weak staining in < 10% of the cells; 1, weak staining in >40% or moderate staining in 10-40% of the cells; 2, moderate staining in >40% or strong staining in 10-40% of the cells and 3, strong staining in >40% of the cells.⁴⁷

Total and nuclear protein extraction and western blots—Total protein was extracted using lysis buffer from Cell Signaling Technology (cat# 9803) per the manufacturer's protocols. Nuclear and cytosolic proteins were prepared using NE-PER Nuclear and Cytosolic Extraction Reagents (cat# 78833, Pierce biotechnology, Rockford, IL). Protein concentration was quantified by Bradford assay (Bio-Rad Laboratories, Hercules, CA). Aliquots of 50 µg of total protein or 20 µg nuclear protein were resolved by SDS-PAGE and transferred onto polyvinylidene difluoride membranes. The blots were blocked in Blotto-Tween solution (5% nonfat dry milk, 0.05% Tween in PBS) for 1 hour and then incubated in Blotto-Tween with the primary antibodies (Supplementary Data 1) for 2 hours at room temperature. For loading control, the membranes were stripped and re-probed with mouse anti-GAPDH for total protein, or rabbit anti-TFIID antibody for nuclear protein. Labeled protein was visualized by using a chemiluminescence detection system (ECL, Amersham, Piscataway, NJ).

Quantitative Reverse Transcription polymerase chain reaction—Briefly, we prepared 250 ng of total RNA using Trizol, RNazol (Molecular Research Center, Cincinnati, OH, catalog# RN190) and reverse transcribed using the iScript™ cDNA Synthesis Kit (BioRad, Hercules CA, catalog #170-8891), Real time PCR was performed with SsoFast™ EvaGreen® Supermix, (BioRad, Hercules CA, catalog #1725201) according to the manufacturer's protocol and as previously described.^{35, 46} Primers were designed and manufactured by Integrated DNA Technologies (Coralville, IA). Sequences are listed in Supplementary Data 1. We normalized expression using GAPDH as internal control. Each primer set included a minus RT control and negative template control. Triplicates of each sample were used for qPCR reactions. Subsequent data analyses were performed using the average Cq for each sample. Fold changes were calculated by the delta-delta Cq method in which the expression of the PCR product was compared to the Cq value of an arbitrarily chosen sample (in this case one of the NERD samples) as we did previously.³⁵ Thus, all fold changes were in relation to the Cq value in that sample.

Epithelial to mesenchymal transition and cell motility assays—Epithelial to mesenchymal transition (EMT) was measured by immunostaining for epithelial markers such as E-cadherin and mesenchymal markers such as vimentin and Snail as we did previously.⁴⁴ EMT was defined by decreased expression of E-cadherin and increased expression of vimentin and Snail. Previously described scratch assay was used to determine

the effect of *FOXF1* gene on EPC2 cell motility.⁴⁴ At 70-80 % confluency, scratch wounds were made in the EPC2 cells (*FOXF1*-transfected and vector-transfected) using a pipette tip. Scratched areas were photographed at 0h, 6h and 12h using a phase contrast inverted microscope (Axiovert 100 TV, Carl Zeiss AG, Oberkochen, Germany). Objective analysis in arbitrary units was performed using automated image function in Photoshop v. 20.0.8. The measurement scale function turns the entire image into a grid with X and Y coordinates. Using the ruler tool, a line was drawn across the wound. The wound width was then calculated as the difference between the two X coordinates of that line. These measurements were made at three locations along the wound length and the mean values were used for analyses.

Next generation sequencing and Pathway analysis

RNA was extracted using RNazol reagent (Molecular Research Center, Cincinnati, OH). Total RNA sequencing was performed in an Illumina HiSeq 2500 sequencing machine (Illumina, San Diego, CA) at a 2×100 bp paired-end resolution. Details of library preparation are provided under Supplementary Data 1. The strand-specific sequenced reads were mapped to the human genome (GRCh38) using the STAR software.⁴⁸ Transcript abundance estimates were calculated using the HTSeq software.⁴⁹ The resulting gene expression counts were analyzed using a Negative Binomial generalized linear model (NB-GLM) from the edgeR package⁵⁰ to identify statistically significant differentially expressed genes. The significance p-values were adjusted for multiple hypotheses testing by the Benjamini and Hochberg method. Biological functional and pathway analysis was performed using Ingenuity Pathway Analysis (IPA) software (QIAGEN Inc., ingenuitypathway-analysis).

Statistical analysis

Interobserver agreement between pathologists for FOXF1 protein expression was measured by calculating Kappa values (κ) with 95% confidence intervals.⁵¹ Kappa values reflect the degree of agreement: 0-0.2=poor, 0.2-0.4=fair, 0.4-0.6=moderate, 0.6-0.8=substantial and 0.8-1.0=excellent. ANOVA was used for multiple group comparisons. Post ANOVA Pairwise comparisons were performed by Student's t-test. All analyses were performed using GraphPad v8.3.0. A *P* value of <.05 was considered significant.

Results

FOXF1 was uniquely expressed in the columnar epithelium of BE

FOXF1 transcript and protein levels were evaluated in biopsy specimens from patients with GERD (n=40, 20 with erosive esophagitis (EE) and 20 with non-erosive reflux disease (NERD) and BE (n=20) (Table 1). Additionally, we examined the squamous esophagus of BE patients at a distance of two cm from the proximal edge of BE. Quantitative PCR showed *FOXF1* expression to be seven-fold higher in Barrett's epithelium compared to the squamous epithelium of patients with NERD and EE and to the paired squamous epithelium of patients with BE, all *P*<.01 (Figure 1).

FOXF1 protein expression was evaluated by IHC. All slides were reviewed by two pathologists. The interobserver agreement between pathologists for various comparisons was moderate to substantial with kappa values ranging from 0.41-0.86. The proportion of patients with epithelial FOXF1 expression was significantly higher in BE patients compared to GERD patients (85% versus 15%, $P=0.01$ for both) (Figure 1). Similarly, the proportion of patients with stromal FOXF1 expression was significantly higher in BE patients versus GERD patients (90% versus 10%, $P=0.01$ for both) (data not shown). The above results demonstrate that *FOXF1* is strongly expressed in columnar epithelium compared to squamous epithelium.

Acid and bile upregulated *FOXF1* in multiple normal esophageal squamous cell lines

Established in-vitro models of BE pathogenesis were used.⁵² Given that there is no universal agreement on acid and bile concentrations for in vitro experiments, dose and duration based tests were performed. EPC2 cells were exposed to incremental doses of acid alone and acidic bile salts for varying durations (Supplementary Data 1). We found that pH 5.0 or pH 4.0 but not pH 5.5 caused significant cell loss irrespective of duration of exposure. Therefore, we chose pH 5.5 for all experiments. We also found that at pH 5.5, bile salts caused significant cell loss at concentrations higher than 100 μ M irrespective of duration of exposure. Based on these data, we chose the final experimental conditions for acid alone treatment to be pH 5.5 for 30 minutes and acidic bile salt treatment to be bile salt concentration of 100 μ M at pH 5.5 for 30 minutes. When treated under these conditions for 30 minutes, acid as well as acidic bile salts increased *FOXF1* expression in EPC2 and Het-1A cells by IHC (Figure 2A). We then tested two newly established esophageal squamous cell lines, NESB10 from a patient with BE and NESG4 from a patient without BE⁴⁴. Time-based experiments showed that in both NESB10 and NESG4 cells, acidic bile increase nuclear expression of FOXF1 by 10 to 15 minutes (Figure 2B). These results suggest that both acid and acidic bile salts are strong stimuli for induction of *FOXF1* in multiple esophageal squamous cell lines.

FOXF1 overexpression caused human esophageal squamous cells to acquire a BE like columnar phenotype based on molecular markers, organoid structure and global gene profiles

Changes in molecular markers—We examined the effects of *FOXF1* transfection in EPC2 esophageal squamous cells in dose-ranging experiments. Established columnar and squamous markers were used as endpoints. We transfected *FOXF1* plasmid into normal esophageal cells over a serial dilution by a factor of 10 that caused *FOXF1* expression to change from 13-fold to 100,000-fold (data not shown). We found that the plasmid dose of 0.0004 μ g increased FOXF1 expression by 13-fold (data not shown) that approximates the degree of fold change (~7-fold) seen in BE epithelium compared to squamous epithelium. This dose was used for all subsequent experiments. We found that at all of these fold changes, *FOXF1* transfection increased columnar cytokeratins 18 and 7 and decreased squamous cytokeratins 10 and 13 suggesting high potency of *FOXF1* (Figure 3). We then used lentiviral vectors to stably overexpress *FOXF1* in NES-G4 esophageal squamous cells (Figure 4A). *FOXF1* overexpression induced well-known columnar cytokeratins, CK18 and

CK7 and a BE differentiation marker, mucin 2, in NES-G4 esophageal squamous cells (Figure 4B, 4C).

Organoid culture—Organoids of normal esophageal squamous epithelial cells were spherical structures as shown in previous publications.⁴⁵ When these cells were stably transfected with *FOXF1*, the organoids developed budding structures similar to budding projections seen in previous studies⁵³ for columnar glandular epithelium (Figure 4D).

Global gene profiles after FOXF1 transfection—*FOXF1* is a pioneer factor^{30, 31} and can cause profound changes in cellular gene expression. Therefore, we assessed whether changes in *in vitro* global gene expression profiles after *FOXF1* transfection correlated with the differences in *in vivo* global gene profiles between BE and GERD patients. Using RNA sequencing, we found that genes that were highly upregulated after *FOXF1* transfection *in vitro* were also highly differentially upregulated between BE and GERD patients ($P=2.1685e-06$) *in vivo* and genes that were highly downregulated after *FOXF1* transfection *in vitro* were also highly differentially downregulated between BE and GERD patients ($P=8.3378e-09$) *in vivo* (Table 2). Raw *in vitro* data are available at GEO accession # GSE122481. The analyzed patient sequencing data are available as Supplementary Data 2. Together, the above results support a strong relationship between *FOXF1* gene expression and initiation of a columnar type phenotype

Foxf1 inhibition in Barrett's cells led to reduced expression of BE differentiation markers

We then asked whether *FOXF1* was important for maintaining the differentiation status of BE. We chose two well-known BE differentiation markers, CK7 and Muc2. Muc2 is highly expressed in goblet cells that are the hallmark of BE epithelium.⁵⁴ BAR-T cells were transfected with four distinct *FOXF1* shRNA clones. Although the clones B, C & D led to inhibition of *FOXF1*, only clones C & D resulted in reduced expression of the BE molecular marker CK7 (Fig. 5A). Alignment of the shRNA clones to the UCSC genome browser (GRCh38/hg38, Dec 13)⁵⁵ showed that unlike clones C and D with 100% specificity to *FOXF1*, clone B shRNA had 89% hit in chromosome 6 to FoxQ1, another member of the FOX family, with as yet undefined interactions with *FOXF1*. This could explain discrepant results caused by shRNA clone B. For further confirmation, we used immunofluorescence to show that both clones C & D reduced BE molecular markers i.e., Muc2 and CK7 (Fig. 5B and 5C). These experiments suggest that *FOXF1* is important for the maintenance of the columnar BE epithelium.

FOXF1 induced EMT in esophageal squamous epithelial cells

Thus far, we determined that *FOXF1* is intricately tied to maintenance of a columnar phenotype. Based on our previous publication,⁴⁴ we hypothesized that *FOXF1* may promote migration of primed squamous cells from their native location to escape pro-squamous stimuli and differentiate into columnar cells in a new environment. We evaluated *FOXF1*-transfected esophageal squamous cells, EPC2, for EMT (Figure 6A). We found that the expression of E-cadherin decreased while the expression of vimentin and Snail increased in the *FOXF1*-transfected cells but not in the vector-transfected cells. Next, cell motility assays were performed (Figure 6B). At both 6 and 12 hours, cells migration was more in *FOXF1*

transfected cells compared to vector-transfected cells. Translating these results clinically, these results suggest that *FOXF1* could promote migration of esophageal squamous cells to populate reflux-induced esophageal wounds while committing them to a columnar fate to promote Barrett's like metaplasia.

Pathway analysis

To investigate the pathways regulated by *FOXF1*, we used RNAseq to measure gene expression after *FOXF1* transfection (data deposited at GEO accession # GSE122481). *FOXF1* expression *in vitro* increased by 8.9-fold that closely approximates the 7-fold change in expression seen *in vivo* in BE compared to GERD. At a threshold of FDR *P* value <0.05, a total of 776 genes were upregulated and 594 genes were down-regulated. The IPA analysis identified a total of 9 networks. Table 3 lists the top 3 networks that were comprised of both upregulated and downregulated genes. One of the top networks was “*Cancer, Cellular Assembly and Organization, DNA Replication, Recombination, and Repair*” that has not been linked to BE development. Previous data showed the BE mutational load to be high (2.8 mutations/Mb), even before progression to invasive cancer, which is comparable to that seen in many common invasive cancers such as prostate and breast.⁵⁶ Conventionally, DNA repair pathways are believed to be dysregulated later in the process of carcinogenesis⁵⁷ but our data raise the possibility that dysregulated DNA repair pathways may be an early event in BE.

Discussion

FOXF1 is uniquely and consistently linked to BE development and progression based on multiple genetic epidemiology studies.⁹⁻¹⁷ However, direct evidence for the role of *FOXF1* in determining cell fate during squamous to columnar metaplasia has been lacking. To the best of our knowledge, this is the first study confirming the functional relevance of *FOXF1* in the pathogenesis of BE and validates the findings of genetic epidemiology studies. *FOXF1* should be further studied as a useful diagnostic marker and as a therapeutic target in BE.

Multiple BE development models have been proposed: transdifferentiation of native terminally differentiated squamous cells to columnar cells, transcommitment of progenitor squamous cells or cells from the submucosal glands to a specialized BE epithelium⁵⁸ and wound repair model with migration of glandular cells⁸ or transitional cells⁶ or residual embryonic cells from the gastric cardia⁷ or diapiesis of circulating bone marrow-derived cells.⁵⁹ Our data favor the transcommitment model. We tested multiple esophageal squamous cell lines, EPC2, Het-1A, NES-B10 and NES-G4 cells. All of the esophageal squamous cell lines were patient-derived. Our results were consistent across multiple cell lines. To confidently detect the transition from squamous to columnar after *FOXF1* expression, we evaluated well-established squamous and columnar markers, compared *in vitro* global gene expression profiles to patient-based gene expression profiles in GERD and BE and evaluated the change in organoid structure. We found that in our *in vitro* models, *FOXF1*-transfected esophageal squamous cells expressed columnar cytokeratins seen in BE, exhibited changes in gene expression that correlated with *in vivo* BE patient

samples and developed tubular, glandular structures reminiscent of BE glandular epithelium (Figure 4). Our study design also involved unique dose ranging experiments that have not been typically performed while evaluating the effects of transcription factors in squamous to columnar transition. These dose-ranging experiments showed high potency of *FOXF1*-induced effects (Figure 3). To demonstrate the necessity of *FOXF1* in maintaining the columnar phenotype of BE, we used a combination of shRNA clones to inhibit *FOXF1* in a BE cell line, BAR-T. When we inhibited *FOXF1*, well-known Barrett's epithelial markers, mucin 2 and cytokeratin 7, decreased tremendously (Figure 5). The metaplastic initiation was accompanied by global gene expression changes in 776 upregulated and 594 downregulated genes (Table 2) as would be expected for a major epithelial switch and these genes regulated multiple important pathways (Table 3). Together these data strongly support an important role for *FOXF1* in BE development.

FOXF1 was recently recognized to be a pioneer factor^{30, 31} based on experimental observations that it can prime genes for expression by modulating chromatin accessibility, thereby, allowing other transcription factors to change gene expression to determine cell fate. Future studies should investigate *FOXF1*-induced changes in the chromatin state by using techniques such as Chip-Seq and ATAC-seq. These could help us understand the DNA binding sites and open and closed chromatin sites for *FOXF1* to elucidate the mechanisms by which *FOXF1* influences transcription during BE development. *FOXF1* has other important roles that could support an important role in squamous to columnar metaplasia. There are multiple Gli binding sites in the non-coding regions close to *FOXF1*, several of which are evolutionary conserved.²⁰ Thus, *FOXF1* could mediate the effects of hedgehog signaling, a pathway important to BE development, which in turn is regulated by BMP signaling. Pathway analysis implicated DNA damage repair pathways in BE development (Table 3). The concepts around BE progression are changing. Recent data show that instead of slow stepwise progression, BE may rapidly progress to invasive cancer over 24-48 months by catastrophic chromosomal damage.⁶⁰ Based on the pathway analysis of our data, where as many as 50% of the genes were altered in the network *Cancer, Cellular Assembly and Organization, DNA Replication, Recombination, and Repair*, it is possible that these pathways are altered early during BE development and thus prime BE epithelium to undergo neoplastic transformation.

A novel finding of our work was that over-expression of *FOXF1* in normal esophageal squamous cells induced EMT that promoted cell motility. It is plausible that squamous cells from the edges of reflux-induced wounds could migrate into areas of epithelial loss where pro-columnar stromal signaling may revert these *FOXF1*-primed cells into an embryonic columnar state. Our results are consistent with a study by Roudebush et al. in which acid and bile exposure increased migration of esophageal squamous cells to lead to wound repair and tissue regeneration.⁶¹ We previously showed that acid and bile salts induce EMT in non-neoplastic Barrett's BAR-T cells by VEGF signaling⁴⁴ predisposing to the development of sub-squamous intestinal metaplasia in BE. The results of our current experiments are in contrast to our previous publication where acid and bile treatment of normal esophageal squamous cells did not induce EMT, even though our current experiments showed that acid and bile robustly induced *FOXF1*. It is possible that EMT induction needs sustained rather than transient expression of *FOXF1*. Induction of EMT is consistent with the embryological

behavior of FOXF1. Embryologically, *FOXF1* is expressed in the splanchnic mesoderm and is critical for EMT signaling during gut development.⁶² Clinically, if one can imagine a 10 cm long segment of BE, transcommitted squamous cells migrating locally from the edges of the reflux-induced esophageal wounds may be more efficient than migration of cells (transitional cells⁶ or residual embryonic cells⁷) from the gastroesophageal junction across a distance of 10 cm into the proximal esophagus. Thus, our work favors transcommitment as a model for BE development, but we cannot exclude the possibility that *FOXF1* may promote cell motility in other cell types such as transitional or residual embryonic cells to promote migration of these cells proximally from the gastroesophageal junction.

The major strengths of our study were that we included human material as well as *in vitro* cell-culture and organoid models and performed gain-of-function and loss-of-function studies. We chose robust endpoints: specific cytokeratin markers, global gene profiling and change in organoid structure. We also studied the relationship between these markers with the dose of *FOXF1* that provides additional confidence into our observations. Our study does have limitations but overall supports the findings of genetic epidemiology studies that support *FOXF1* as an important factor in the development of BE. Our study population was dominated by males because the patients were enrolled at a Veterans' hospital with male predominance. We do not have reason to suspect sex-based differences in *FOXF1* expression, but our findings should be evaluated in females with BE. We did not study transgenic mice to evaluate the effects of *FOXF1* knockout on BE development and progression. We plan to study the effects on BE development by performing reflux-inducing surgeries in *FOXF1* knockout mice. We discovered specific downstream targets such as PPM1H but could not elucidate them further, which should be done in future studies. The FOXF1-transfected cells grew into organoids with budding structures similar to organoids grown from human BE epithelium by other groups.⁵³ However, we did not observe other characteristics such as central lumen, columnar orientation, surface microvilli and loss of intracellular bridging. It is possible that *FOXF1* initiates early metaplastic change in squamous cells, but other factors may be needed for fully developed BE organoids. We did not study whether *FOXF1* is constitutively expressed in the normal intestinal epithelium. The physiologic (in small intestine and large intestine) versus pathologic (in BE) expression of *FOXF1* should be further studied.

In conclusion, using established *in vitro* models and clinical samples, we have shown that *FOXF1* may play an important role during BE development. Further research is needed to understand whether *FOXF1* can be a novel biomarker to identify GERD patients at risk for BE and whether therapies targeted at *FOXF1* can be used for cancer prevention in patients with BE.

Supplementary Material

Refer to Web version on PubMed Central for supplementary material.

Acknowledgment

This project was supported by an Institutional Development Award (IDeA) from the National Institute of General Medical Sciences of the National Institutes of Health under grant number P20 GM103418 (LKC, AB). The content

is solely the responsibility of the authors and does not necessarily represent the official views of the National Institute of General Medical Sciences or the National Institutes of Health. MS received support, in part, from NIH/NIDDK R01DK107490 and VA BX001037. The Ingenuity Pathways Analysis (IPA) software used in this publication was supported by the Biostatistics and Informatics Shared Resource, funded by the National Cancer Institute Cancer Center Support Grant P30 CA168524, and the Kansas IDeA Network of Biomedical Research Excellence Bioinformatics Core, supported in part by the National Institute of General Medical Science award P20GM103418. RNA sequencing was performed by the Genomics core supported by the Genomics Core at the University of Kansas Medical Center supported by Kansas Intellectual and Developmental Disabilities Research Center (NIH U54 HD 090216), the Molecular Regulation of Cell Development and Differentiation – COBRE (P30 GM122731-03) - the NIH S10 High-End Instrumentation Grant (NIH S10OD021743) and the Frontiers CTSA grant (UL1TR002366). We also acknowledge the contribution of Dr. Ossama Tawfik at the University of Kansas for his willingness to serve as the second gastrointestinal pathologist for the study.

Abbreviations:

FOXF1	Forkhead box F1
GERD	Gastroesophageal Reflux Disease
BE	Barrett's esophagus
EAC	esophageal adenocarcinoma
EMT	epithelial-mesenchymal transition

References

1. Thrift AP. Determination of risk for Barrett's esophagus and esophageal adenocarcinoma. *Current opinion in gastroenterology* 2016;32(4):319–324. [PubMed: 27276368]
2. Islami F, DeSantis CE, Jemal A. Incidence Trends of Esophageal and Gastric Cancer Subtypes by Race, Ethnicity, and Age in the United States, 1997-2014. *Clin Gastroenterol Hepatol* 2019;17(3):429–439. [PubMed: 29902641]
3. Arnold M, Laversanne M, Brown LM, et al. Predicting the Future Burden of Esophageal Cancer by Histological Subtype: International Trends in Incidence up to 2030. *The American journal of gastroenterology* 2017;112(8):1247–1255. [PubMed: 28585555]
4. Spechler SJ, Souza RF. Barrett's esophagus. *N Engl J Med* 2014;371(9):836–845. [PubMed: 25162890]
5. Quante M, Bhagat G, Abrams JA, et al. Bile acid and inflammation activate gastric cardia stem cells in a mouse model of Barrett-like metaplasia. *Cancer Cell* 2012;21(1):36–51. [PubMed: 22264787]
6. Jiang M, Li H, Zhang Y, et al. Transitional basal cells at the squamous-columnar junction generate Barrett's oesophagus. *Nature* 2017;550(7677):529–533. [PubMed: 29019984]
7. Wang X, Ouyang H, Yamamoto Y, et al. Residual embryonic cells as precursors of a Barrett's-like metaplasia. *Cell* 2011;145(7):1023–1035. [PubMed: 21703447]
8. Agoston AT, Pham TH, Odze RD, et al. Columnar-Lined Esophagus Develops via Wound Repair in a Surgical Model of Reflux Esophagitis. *Cell Mol Gastroenterol Hepatol* 2018;6(4):389–404. [PubMed: 30186929]
9. Su Z, Gay LJ, Strange A, et al. Common variants at the MHC locus and at chromosome 16q24.1 predispose to Barrett's esophagus. *Nature genetics* 2012;44(10):1131–1136. [PubMed: 22961001]
10. Becker J, May A, Gerges C, et al. Supportive evidence for FOXP1, BARX1, and FOXF1 as genetic risk loci for the development of esophageal adenocarcinoma. *Cancer Med* 2015;4(11):1700–1704. [PubMed: 26383589]
11. Dura P, van Veen EM, Salomon J, et al. Barrett associated MHC and FOXF1 variants also increase esophageal carcinoma risk. *Int J Cancer* 2013;133(7):1751–1755. [PubMed: 23504527]
12. Lam C, Liu WF, Bel RD, et al. Polymorphisms of the FOXF1 and MHC locus genes in individuals undergoing esophageal acid reflux assessments. *Dis Esophagus* 2017;30(2):1–7.

13. Levine DM, Ek WE, Zhang R, et al. A genome-wide association study identifies new susceptibility loci for esophageal adenocarcinoma and Barrett's esophagus. *Nat Genet* 2013;45(12):1487–1493. [PubMed: 24121790]
14. Palles C, Chegwidzen L, Li X, et al. Polymorphisms near *TBX5* and *GDF7* are associated with increased risk for Barrett's esophagus. *Gastroenterology* 2015;148(2):367–378. [PubMed: 25447851]
15. Palles C, Findlay JM, Tomlinson I. Common Variants Confer Susceptibility to Barrett's Esophagus: Insights from the First Genome-Wide Association Studies. *Adv Exp Med Biol* 2016;908:265–290. [PubMed: 27573776]
16. Su Z, Gay LJ, Strange A, et al. Common variants at the MHC locus and at chromosome 16q24.1 predispose to Barrett's esophagus. *Nat Genet* 2012;44(10):1131–1136. [PubMed: 22961001]
17. van Nistelrooij AM, van der Korput HA, Broer L, et al. Single nucleotide polymorphisms in *CRTC1* and *BARX1* are associated with esophageal adenocarcinoma. *J Carcinog* 2015;14:5. [PubMed: 26085818]
18. Zhang J, Chen J, Ma T, et al. Genetic variants of *FOXP1* and *FOXF1* are associated with the susceptibility of oesophageal adenocarcinoma in Chinese population. *J Genet* 2018;97(1):213–218. [PubMed: 29666340]
19. Lam EW, Brosens JJ, Gomes AR, et al. Forkhead box proteins: tuning forks for transcriptional harmony. *Nat Rev Cancer* 2013;13(7):482–495. [PubMed: 23792361]
20. Madison BB, McKenna LB, Dolson D, et al. FoxF1 and FoxL1 link hedgehog signaling and the control of epithelial proliferation in the developing stomach and intestine. *J Biol Chem* 2009;284(9):5936–5944. [PubMed: 19049965]
21. Shaw-Smith C Genetic factors in esophageal atresia, tracheo-esophageal fistula and the VACTERL association: roles for *FOXF1* and the 16q24.1 FOX transcription factor gene cluster, and review of the literature. *Eur J Med Genet* 2010;53(1):6–13. [PubMed: 19822228]
22. Vergouwe FWT HIJ, Biermann K, et al. High Prevalence of Barrett's Esophagus and Esophageal Squamous Cell Carcinoma After Repair of Esophageal Atresia. *Clin Gastroenterol Hepatol* 2018;16(4):513–521 e516. [PubMed: 29133255]
23. Wang DH, Clemons NJ, Miyashita T, et al. Aberrant epithelial-mesenchymal Hedgehog signaling characterizes Barrett's metaplasia. *Gastroenterology* 2010;138(5):1810–1822. [PubMed: 20138038]
24. Clemons NJ, Wang DH, Croagh D, et al. Sox9 drives columnar differentiation of esophageal squamous epithelium: a possible role in the pathogenesis of Barrett's esophagus. *Am J Physiol Gastrointest Liver Physiol* 2012;303(12):G1335–1346. [PubMed: 23064761]
25. Kazumori H, Ishihara S, Kinoshita Y. Roles of caudal-related homeobox gene *Cdx1* in oesophageal epithelial cells in Barrett's epithelium development. *Gut* 2009;58(5):620–628. [PubMed: 19136512]
26. Kazumori H, Ishihara S, Takahashi Y, et al. Roles of Kruppel-like factor 4 in oesophageal epithelial cells in Barrett's epithelium development. *Gut* 2010.
27. van Baal JW, Verbeek RE, Bus P, et al. microRNA-145 in Barrett's oesophagus: regulating BMP4 signalling via GATA6. *Gut* 2012.
28. di Pietro M, Lao-Sirieix P, Boyle S, et al. Evidence for a functional role of epigenetically regulated midcluster HOXB genes in the development of Barrett esophagus. *Proceedings of the National Academy of Sciences of the United States of America* 2012.
29. Mari L, Milano F, Parikh K, et al. A pSMAD/CDX2 Complex Is Essential for the Intestinalization of Epithelial Metaplasia. *Cell reports* 2014.
30. Lee DM, Duensing A. What's the FOX Got to Do with the KITten? Regulating the Lineage-Specific Transcriptional Landscape in GIST. *Cancer Discov* 2018;8(2):146–149. [PubMed: 29431674]
31. Ran L, Chen Y, Sher J, et al. *FOXF1* Defines the Core-Regulatory Circuitry in Gastrointestinal Stromal Tumor. *Cancer Discov* 2018;8(2):234–251. [PubMed: 29162563]
32. Bansal A, Hong X, Lee IH, Krishnadath KK, Mathur SC, Gunewardena S, Rastogi A, Sharma P, Christenson L. MicroRNA expression can be a promising strategy for the detection of

Barrett's Esophagus: A pilot study Clinical and translational gastroenterology 2014;doi:10.1038/ctg.2014.17 [in press].

33. Bansal A, Lee IH, Hong X, et al. Feasibility of microRNAs as biomarkers for Barrett's Esophagus progression: a pilot cross-sectional, phase 2 biomarker study. *The American journal of gastroenterology* 2011;106(6):1055–1063. [PubMed: 21407181]
34. Montgomery E, Goldblum JR, Greenson JK, et al. Dysplasia as a predictive marker for invasive carcinoma in Barrett esophagus: a follow-up study based on 138 cases from a diagnostic variability study. *Hum Pathol* 2001;32(4):379–388. [PubMed: 11331954]
35. Bansal A, Lee IH, Hong X, et al. Discovery and Validation of Barrett's Esophagus MicroRNA Transcriptome by Next Generation Sequencing. *PLoS ONE* 2013;8(1):e54240. [PubMed: 23372692]
36. Bansal A, McGregor DH, Anand O, et al. Presence or absence of intestinal metaplasia but not its burden is associated with prevalent high-grade dysplasia and cancer in Barrett's esophagus. *Dis Esophagus* 2014;27(8):751–756. [PubMed: 24165297]
37. Harada H, Nakagawa H, Oyama K, et al. Telomerase induces immortalization of human esophageal keratinocytes without p16INK4a inactivation. *Mol Cancer Res* 2003;1(10):729–738. [PubMed: 12939398]
38. Bus P, Siersema PD, Verbeek RE, et al. Upregulation of miRNA-143, -145, -192, and -194 in esophageal epithelial cells upon acidic bile salt stimulation. *Dis Esophagus* 2014;27(6):591–600. [PubMed: 24006894]
39. Jaiswal KR, Morales CP, Feagins LA, et al. Characterization of telomerase-immortalized, non-neoplastic, human Barrett's cell line (BAR-T). *Dis Esophagus* 2007;20(3):256–264. [PubMed: 17509124]
40. Zhang HY, Zhang X, Chen X, et al. Differences in activity and phosphorylation of MAPK enzymes in esophageal squamous cells of GERD patients with and without Barrett's esophagus. *Am J Physiol Gastrointest Liver Physiol* 2008;295(3):G470–478. [PubMed: 18617556]
41. Vaezi MF, Richter JE. An ambulatory bilirubin monitoring device for duodenogastroesophageal reflux. *Surg Technol Int* 1996;5:125–130. [PubMed: 15858728]
42. Nehra D, Howell P, Williams CP, et al. Toxic bile acids in gastro-oesophageal reflux disease: influence of gastric acidity. *Gut* 1999;44(5):598–602. [PubMed: 10205192]
43. Kauer WK, Peters JH, DeMeester TR, et al. Composition and concentration of bile acid reflux into the esophagus of patients with gastroesophageal reflux disease. *Surgery* 1997;122(5):874–881. [PubMed: 9369886]
44. Zhang Q, Agoston AT, Pham TH, et al. Acidic Bile Salts Induce Epithelial to Mesenchymal Transition via VEGF Signaling in Non-Neoplastic Barrett's Cells. *Gastroenterology* 2019;156(1):130–144 e110. [PubMed: 30268789]
45. Kasagi Y, Chandramouleeswaran PM, Whelan KA, et al. The Esophageal Organoid System Reveals Functional Interplay Between Notch and Cytokines in Reactive Epithelial Changes. *Cell Mol Gastroenterol Hepatol* 2018;5(3):333–352. [PubMed: 29552622]
46. De A, Powers B, De A, et al. *Emblica officinalis* extract downregulates pro-angiogenic molecules via upregulation of cellular and exosomal miR-375 in human ovarian cancer cells. *Oncotarget* 2016;7(21):31484–31500. [PubMed: 27129171]
47. Gialmanidis IP, Bravou V, Petrou I, et al. Expression of Bmi1, FoxF1, Nanog, and gamma-catenin in relation to hedgehog signaling pathway in human non-small-cell lung cancer. *Lung* 2013;191(5):511–521. [PubMed: 23864317]
48. Dobin A, Davis CA, Schlesinger F, et al. STAR: ultrafast universal RNA-seq aligner. *Bioinformatics* 2013;29(1):15–21. [PubMed: 23104886]
49. Anders S, Pyl PT, Huber W. HTSeq—a Python framework to work with high-throughput sequencing data. *Bioinformatics* 2015;31(2):166–169. [PubMed: 25260700]
50. Robinson MD, McCarthy DJ, Smyth GK. edgeR: a Bioconductor package for differential expression analysis of digital gene expression data. *Bioinformatics* 2010;26(1):139–140. [PubMed: 19910308]
51. Landis JR, Koch GG. The measurement of observer agreement for categorical data. *Biometrics* 1977;33(1):159–174. [PubMed: 843571]

52. Bus P, Siersema PD, van Baal JW. Cell culture models for studying the development of Barrett's esophagus: a systematic review. *Cell Oncol (Dordr)* 2012;35(3):149–161. [PubMed: 22476962]
53. Sato T, Stange DE, Ferrante M, et al. Long-term expansion of epithelial organoids from human colon, adenoma, adenocarcinoma, and Barrett's epithelium. *Gastroenterology* 2011;141(5):1762–1772. [PubMed: 21889923]
54. Goldblum JR. Barrett's esophagus and Barrett's-related dysplasia. *Modern pathology: an official journal of the United States and Canadian Academy of Pathology, Inc* 2003;16(4):316–324. [PubMed: 12692197]
55. Kent WJ, Sugnet CW, Furey TS, et al. The human genome browser at UCSC. *Genome Res* 2002;12(6):996–1006. [PubMed: 12045153]
56. Stachler MD, Taylor-Weiner A, Peng S, et al. Paired exome analysis of Barrett's esophagus and adenocarcinoma. *Nat Genet* 2015;47(9):1047–1055. [PubMed: 26192918]
57. Secrier M, Li X, de Silva N, et al. Mutational signatures in esophageal adenocarcinoma define etiologically distinct subgroups with therapeutic relevance. *Nat Genet* 2016;48(10):1131–1141. [PubMed: 27595477]
58. Biswas S, Quante M, Leedham S, et al. The metaplastic mosaic of Barrett's oesophagus. *Virchows Archiv: an international journal of pathology* 2018;472(1):43–54. [PubMed: 29500519]
59. Sarosi G, Brown G, Jaiswal K, et al. Bone marrow progenitor cells contribute to esophageal regeneration and metaplasia in a rat model of Barrett's esophagus. *Dis Esophagus* 2008;21(1):43–50. [PubMed: 18197938]
60. Li X, Galipeau PC, Paulson TG, et al. Temporal and spatial evolution of somatic chromosomal alterations: a case-cohort study of Barrett's esophagus. *Cancer Prev Res (Phila)* 2014;7(1):114–127. [PubMed: 24253313]
61. Roudebush C, Catala-Valentin A, Andl T, et al. Activin A-mediated epithelial de-differentiation contributes to injury repair in an in vitro gastrointestinal reflux model. *Cytokine* 2019;123:154782. [PubMed: 31369967]
62. Mahlapuu M, Enerback S, Carlsson P. Haploinsufficiency of the forkhead gene *Foxf1*, a target for sonic hedgehog signaling, causes lung and foregut malformations. *Development* 2001;128(12):2397–2406. [PubMed: 11493558]

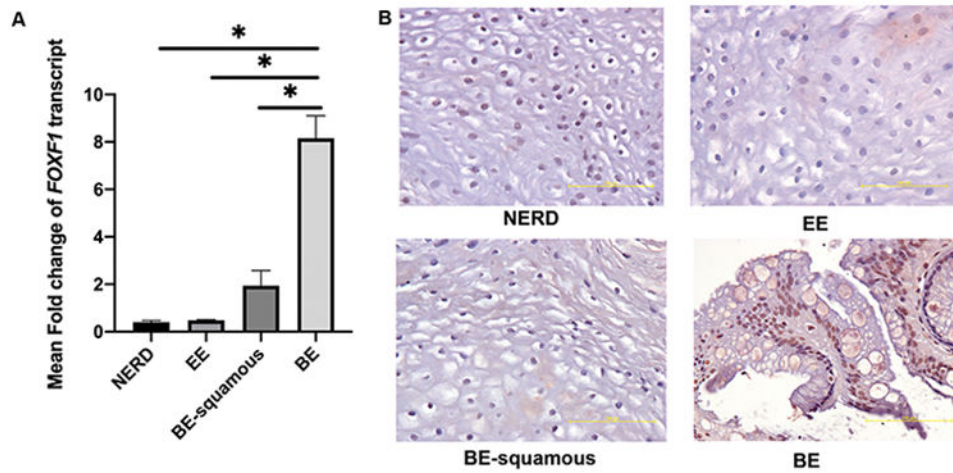


Figure 1. FOXF1 expression in human specimens by qPCR (A) and IHC (B).

FOXF1 transcript and protein (brown staining) was higher in the BE epithelium compared to the squamous epithelium of NERD or EE or BE-squamous. NERD, Non-erosive reflux disease; EE, erosive esophagitis; BE-squamous, paired squamous mucosa from patients with Barrett's esophagus (BE). Fold changes were calculated by the delta-delta Cq method and expressed in comparison to the Cq value of one of the NERD samples. Magnification 40x; Scale bar = 100 μ m. *indicates $P < .01$.

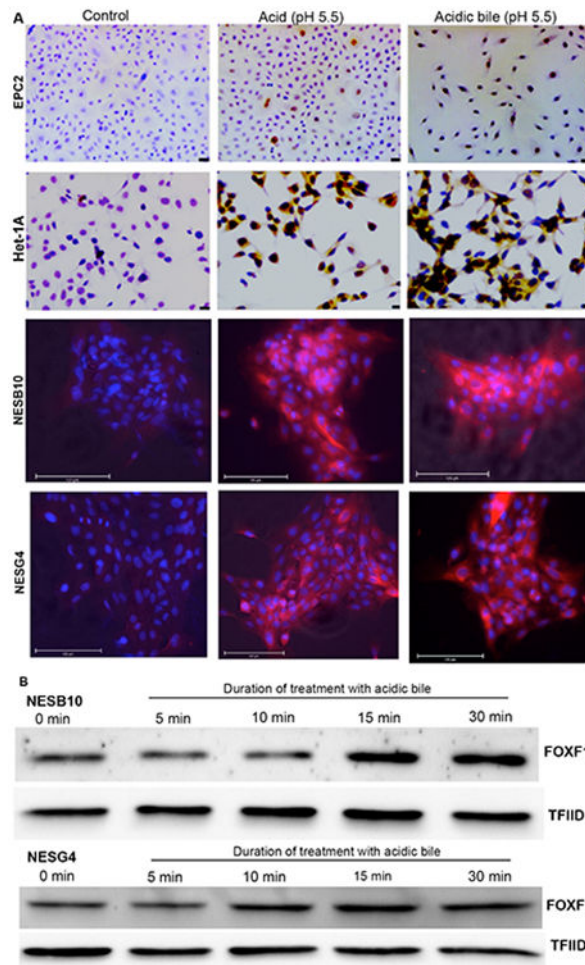
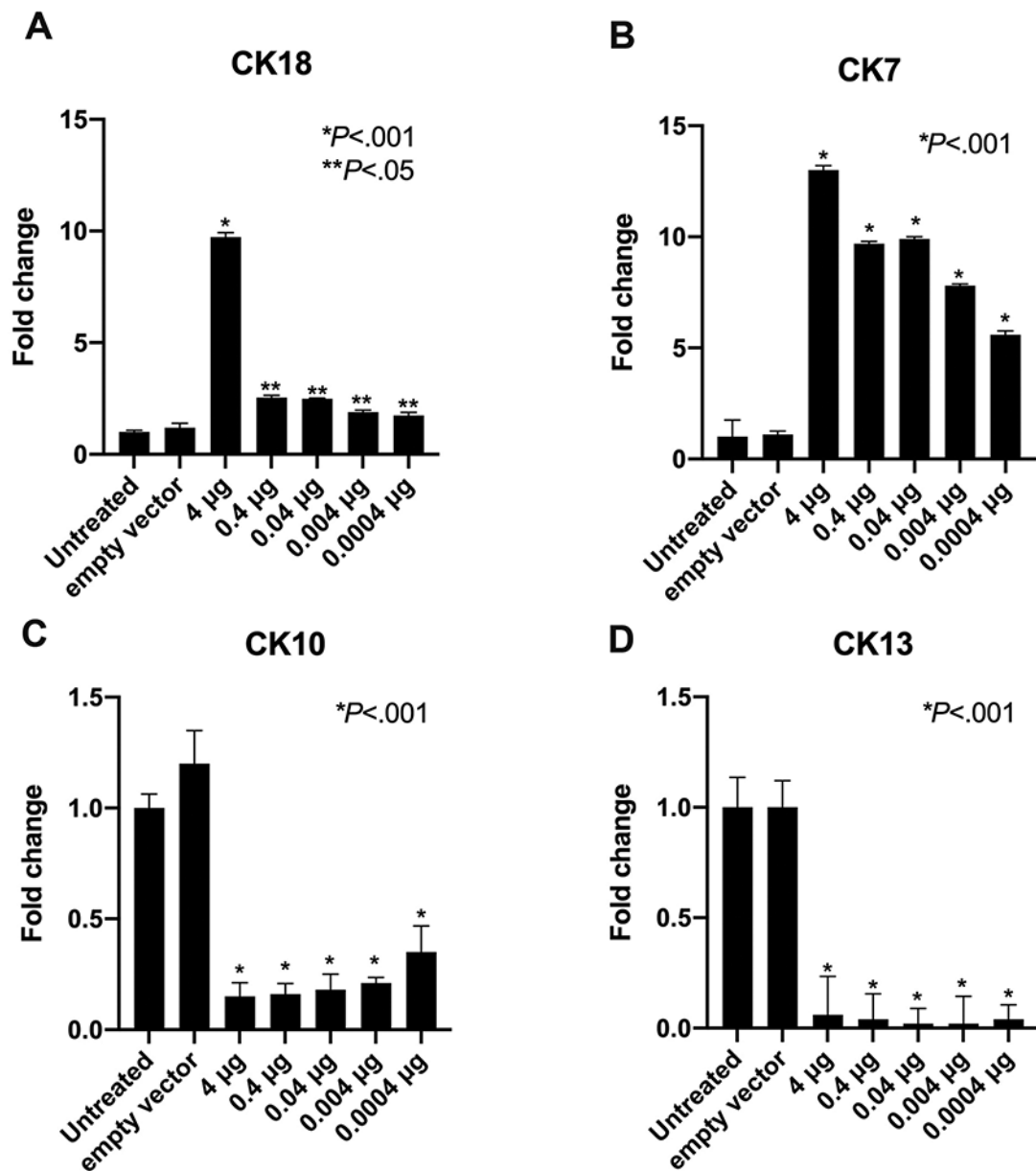


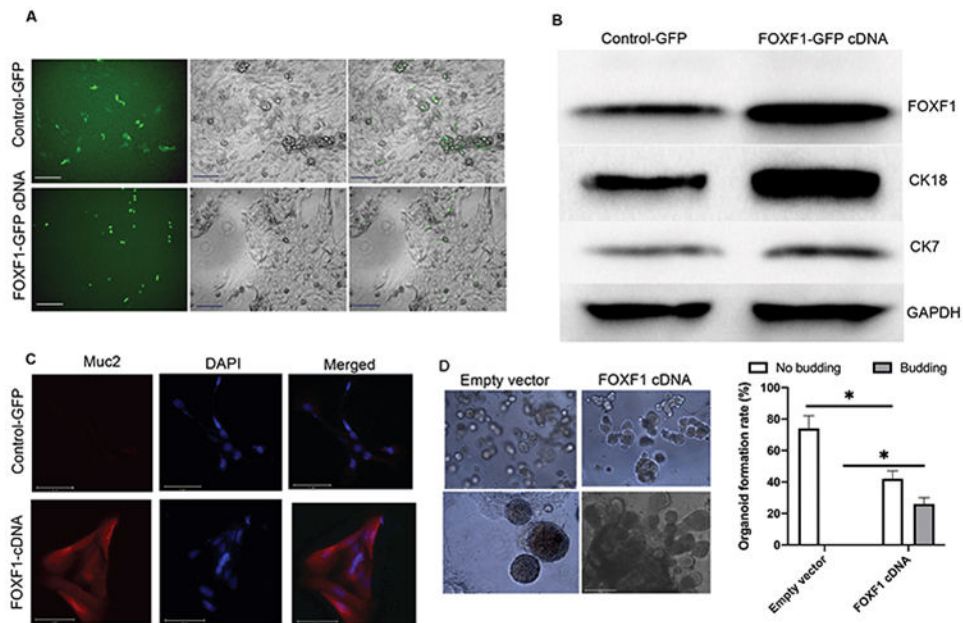
Figure 2. FOXF1 expression after acid and acidic bile treatment.

Four normal esophageal squamous cell lines, EPC2, Het-1A, NESB10 and NESG4 were studied. At 70-80% confluency cells lines were exposed to acid at pH 5.5 and/or acidic bile (bile salts @ 100 μ M at pH 5.5.). In [panel A](#), FOXF1 was evaluated by immunocytochemistry (magnification 20x; scale bar = 24 μ m) or immunofluorescence (scale bar = 125 μ m) after being treated with acid and acidic bile for 30 minutes. In [panel B](#), extracts of nuclear proteins were blotted against FOXF1 after treatment with acidic bile for duration varying from 5 minutes to 30 minutes.



Figures 3. Dose-dependent effects of *FOXF1* on squamous and columnar cytokeratins in normal esophageal squamous EPC2 cells.

At 70% confluency, EPC2 cells were transfected with *FOXF1* at varying doses (0.0004-4 μ g) or empty vector and columnar cytokeratins 18 (A) and 7 (B) and squamous cytokeratins 10 (C) and 13 (D) were measured by qPCR. Data represent mean \pm SEM of four independent experiments.



Figures 4. Effect of *FOXF1* induction on columnar cytokeratins and organoid growth.

Panel A: Lentiviral GFP-tagged empty vector or *FOXF1* cDNA into NESG4 cells led to efficient transduction of *FOXF1*: IF in left panel, phase contrast microscopy in middle panel and merge in right panel. Bar= 75 μ m. **Panel B,** Western blots were performed for columnar cytokeratins, CK18 and CK7, after transfection with lentiviral GFP-tagged empty vector or *FOXF1* cDNA. **Panel C:** IF was performed for Muc2, a well-established BE marker. Scale bar = 50 μ m. **Panels D:** Organoid cultures were established from GFP labeled cells sorted by flow cytometry after transfection with empty vector or *FOXF1* cDNA. Scale bar=50 μ m. The graph shows the proportion of budding organoids between cells transfected with empty vector versus *FOXF1* cDNA, * P <.01.

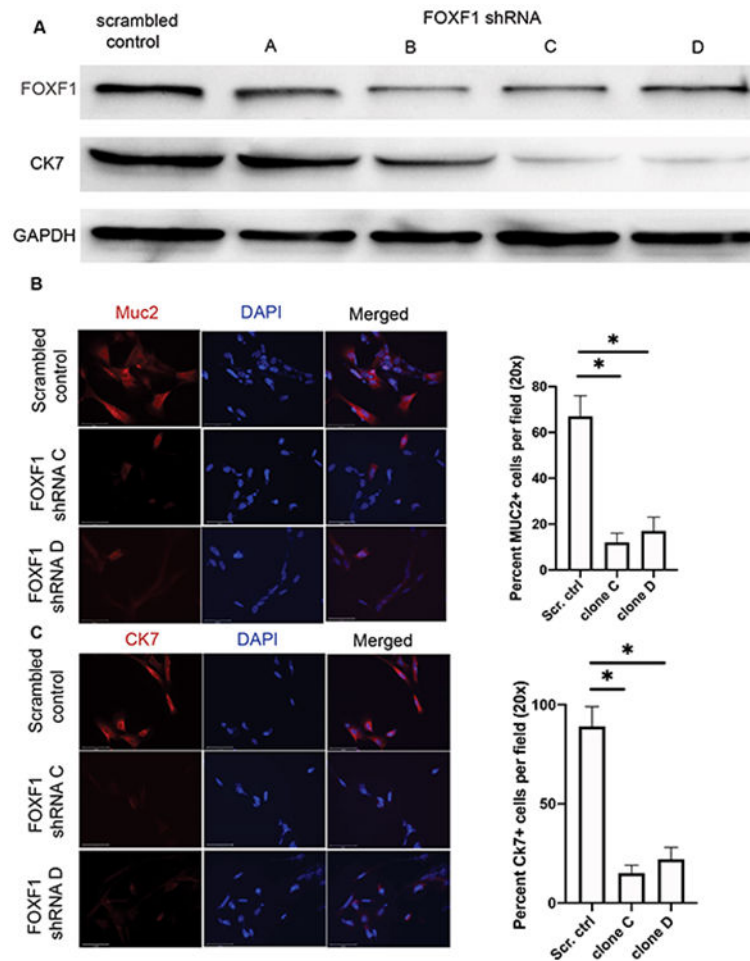


Figure 5. Effects of *FOXF1* inhibition on well-known Barrett's markers in patient-derived Barrett's cells.

Panel A: BAR-T cells were transfected with four different *FOXF1* shRNA clones A-D versus scrambled control and western blots were performed for *FOXF1* and *CK7*. **Panel B** and **C:** BAR-T cells were transfected with the GFP-tagged *FOXF1* shRNA clones C & D and imaged for *Muc2* and *CK7* by confocal microscopy (20x magnification). Scale bar = 50 μ m. Cells were counted from eight random fields for quantitative analysis. Graphs show objective analysis of the fluorescence pictures, * $P < .05$.

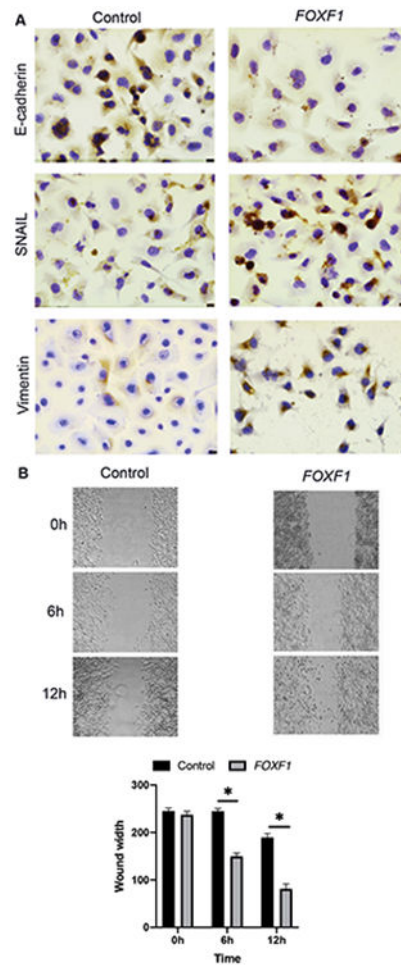


Figure 6. *FOXF1* over-expression induced EMT and promoted cell motility in normal esophageal squamous cells.

EPC2 cells at 70% confluency were transfected with *FOXF1* (0.0004 μ g) or empty vector. Panel A, E-cadherin, Snail and vimentin were evaluated by immunocytochemistry. Panel B, Cell motility assays were performed. Bar graph shows quantification of the wound dimensions using Photoshop arbitrary relative units (see methods), * $P < 0.05$. Data represent mean \pm SEM of three independent experiments. Magnification 20x; Scale bar = 24 μ m.

Table 1.

Patient Demographics

	NERD (n=20)	EE (n=20)	BE (n=20)
<i>Age</i>	59±10.1	61±9.6	63±12.7
<i>Gender</i>	80% male	93% male	95% male
<i>Race</i>	All white	All white	All white
<i>Hiatus Hernia</i>	45%	75%	88%
<i>BMI</i>	27±5.3	29±4.7	32±5.9

NERD, non-erosive reflux disease, EE, erosive esophagitis, BE, Barrett's esophagus

Table 2.

Comparison of changes in gene expression in EPC2 cells after *in vitro* transfection with *FOXF1* compared to empty vector with *in vivo* differences in gene expression between BE and GERD patients

		<i>BE vs. GERD</i>		
		up	down	
<i>Foxf1</i> vs. empty vector	up	246 (2.1685e-06)	84 (1)	776
	down	114 (0.9994)	171 (8.3378e-09)	594
		3154	2482	

BE, Barrett's esophagus, GERD, gastroesophageal reflux disease, up=upregulated genes, down=down-regulated genes. Genes were selected on the basis of FDR *P*value <0.05. For both patient samples and the cell lines (EPC2), three replicates were used. Numbers in red represent genes with a similar pattern of expression *in vitro* and *in vivo* (*P*values are in parentheses).

Pathway analysis

Table 3.

Top Network	Score	Focus molecules	Molecules*
Cell Cycle, Cell-To-Cell Signaling and Interaction, Gene Expression	22	10	6beta-hydroxytestosterone, ABCC8 , Akt, BPHL , CROT , CSHL1 , CUX2 , Cyp2a1, Cyp2a12/Cyp2a22, Cyp2d9 (includes others), DCAF8 , EPO , GCC2 , GHI , GNAQ , HNF4A , HSD11B1 , IGFALS , Insulin, LOC299282 , LTA4H , MT-CYB , MYH7 , NHLRC3 , NRF1 , Proinsulin, RIMS2 , SERP1 , SLC16A14 , Sicolal, TEF , TMEM260 , TOX , UQCRHL , ZNF701
Cellular Function and Maintenance, Developmental Disorder, Neurological Disease	21	10	ADRM1 , AKT1S1 , APLP1 , APP , BCYRN1 , Beta Tubulin, CAD , CALB1 , CAST , CC2D2A , CTH , DAP , DDX21 , DEF6 , DOCK10 , EEF1D , EMB , FMRI , FOS , GRID1 , MMP13 , MT-CYB , PARVA , PEDN4 , POTEE/POTEF , RAC1 , RELA , SEPT2 , STAU1 , TAF11 , TFE3 , TPR , UBA7 , ZNF268 , ZNF449
Cancer, Cellular Assembly and Organization, DNA Replication, Recombination, and Repair	21	10	AKT1S1 , ASPM , ATRX , BCKDHA , CALB1 , CHN1 , COMT , CPE , DBP , DUT , EDA2R , ESR1 , HDAC1 , HDAC4 , HIST1H4J , HSPA13 , mir-183 , MTHFD1 , MYC , NCOA5 , NDRG2 , NFKB (complex), PAX8 , PHLDB2 , PSMB3 , RNF4 , TAF1D , TLE4 , TP53 , TRIM28 , TWIST2 , USP7 , VEZF1 , ZNF10 , ZNF594

* Genes in red were upregulated and genes in green were downregulated. Focus molecules are the "seed" molecules that are predicted to have the most interactions with other genes. The score refers to the total number of molecules that associate with focus molecules in that network.